Petrogenesis and tectonic implications of early Devonian mafic dike–granite association in the northern West Junggar, NW China

Jiyuan Yin, Wen Chen, Wenjiao Xiao, Chao Yuan, Min Sun & Keda Cai

View supplementary material ⧉

Published online: 08 May 2017.

Submit your article to this journal ⧉

View related articles ⧉

View Crossmark data ⧉

Taylor & Francis
Taylor & Francis Group

ARTICLE

Check for updates

Petrogenesis and tectonic implications of early Devonian mafic dike–granite association in the northern West Junggar, NW China

Jiyuan Yin[a], Wen Chen[a], Wenjiao Xiao[b,c,d], Chao Yuan[e], Min Sun[f] and Keda Cai[d]

[a]Laboratory of Isotope Thermochronology, Institute of Geology, Chinese Academy of Geological Sciences, Beijing, China; [b]State Key Laboratory of Lithospheric Evolution, Institute of Geology and Geophysics, Chinese Academy of Sciences, Beijing, China; [c]Chinese Academy of Sciences (CAS), Center for Excellence in Tibetan Plateau Earth Sciences, Beijing, China; [d]Xinjiang Research Center for Mineral Resources, Xinjiang Institute of Ecology and Geography, Chinese Academy of Sciences, Urumqi, China; [e]State Key Laboratory of Isotope Geochemistry, Guangzhou Institute of Geochemistry, Chinese Academy of Sciences, Guangzhou, China; [f]Department of Earth Sciences, The University of Hong Kong, Hong Kong, China

ABSTRACT

Mafic dike–granite associations are common in extensional tectonic settings and important and pivotal in reconstructing crust–mantle geodynamic processes. We report results of zircon U–Pb and hornblende ^{40}Ar-^{39}Ar ages and major-element and trace-element data for mafic dike–granite association from the northern West Junggar, in order to constrain their ages, petrogenesis, and geodynamic process. The mafic dike–granite association was emplaced in the early Devonian. The Xiemisitai monzogranites have high SiO_2 contents and low MgO, Cr, and Ni concentrations, suggesting that they were mainly derived from crustal sources and were probably generated by partial melt of the juvenile mid-lower crust. The mafic dikes have low $Mg^{\#}$ and Cr and Ni abundances, suggesting that they have experienced significant fractional crystallization. The Xiemisitai mafic dikes contain hornblende and biotite and display negative Nb–Ta–Ti anomalies, enrichment of LREEs and LILEs, and depletion of HREEs and HFSEs, consistent with an origin from a lithospheric mantle metasomatized by subducted slab-derived fluids. In addition, the Xiemisitai mafic dikes are plotted within melting trends with little to no garnet (Cpx: Grt = 6:1) in their source. The La/Yb versus Tb/Yb plot also indicates the presence of less than 1% residual garnet in the source region for the Xiemisitai mafic dikes. Therefore, it can be inferred that the Xiemisitai mafic dikes were generated at a correspondingly shallow depth, mostly within the spinel stability field. The Xiemisitai mafic dikes were most probably generated by the partial melting of the metasomatized lithospheric mantle at relatively shallow depths (<80 km). The Xiemisitai mafic dike–granite association could have been triggered by asthenospheric upwelling as a result of the rollback of the subducted Irtysh–Zaysan oceanic lithosphere.

1. Introduction

Mafic dikes commonly occur in crustal extensional environments, and their formation not only implies the orientation of a stress field, but also plays an important role in understanding the geodynamics of important geological events (Halls 1982; Ernst et al. 1995; Park et al. 1995; Ernst and Buchan 2001). They are generally generated from a deep source and are also an important path for transferring magma to the upper crust. Consequently, mafic dikes may provide significant information on the nature of the mantle source, crustal contamination, and geodynamic mechanisms (Weaver and Tarney 1981; Halls 1982). The Central Asian Orogenic Belt (CAOB) is one of the largest accretionary orogenic belts in the Earth and its formation is closely

associated with the evolution and closure of the Palaeo-Asian Ocean (Figure 1(a); Windley et al. 2007; Xiao et al. 2008). It is composed of a complicated collage of various terranes, including island arcs, ophiolites, accretionary prisms, seamounts, and microcontinents (Windley et al. 2007; Kröner et al. 2008; Xiao et al. 2008, 2013; references therein).

As the major components of CAOB (Windley et al. 2007; Xiao et al. 2008), West Junggar and East Kazakhstan both have connected tectonic entities and the same tectonic evolution history, making up the core of the famous Kazakhstan orocline. The Boshchekul–Chingiz arcs can be regarded as the northern limb of the Kazakhstan orocline (Xiao et al. 2010). They may extend eastward to the northern West Junggar (e.g.
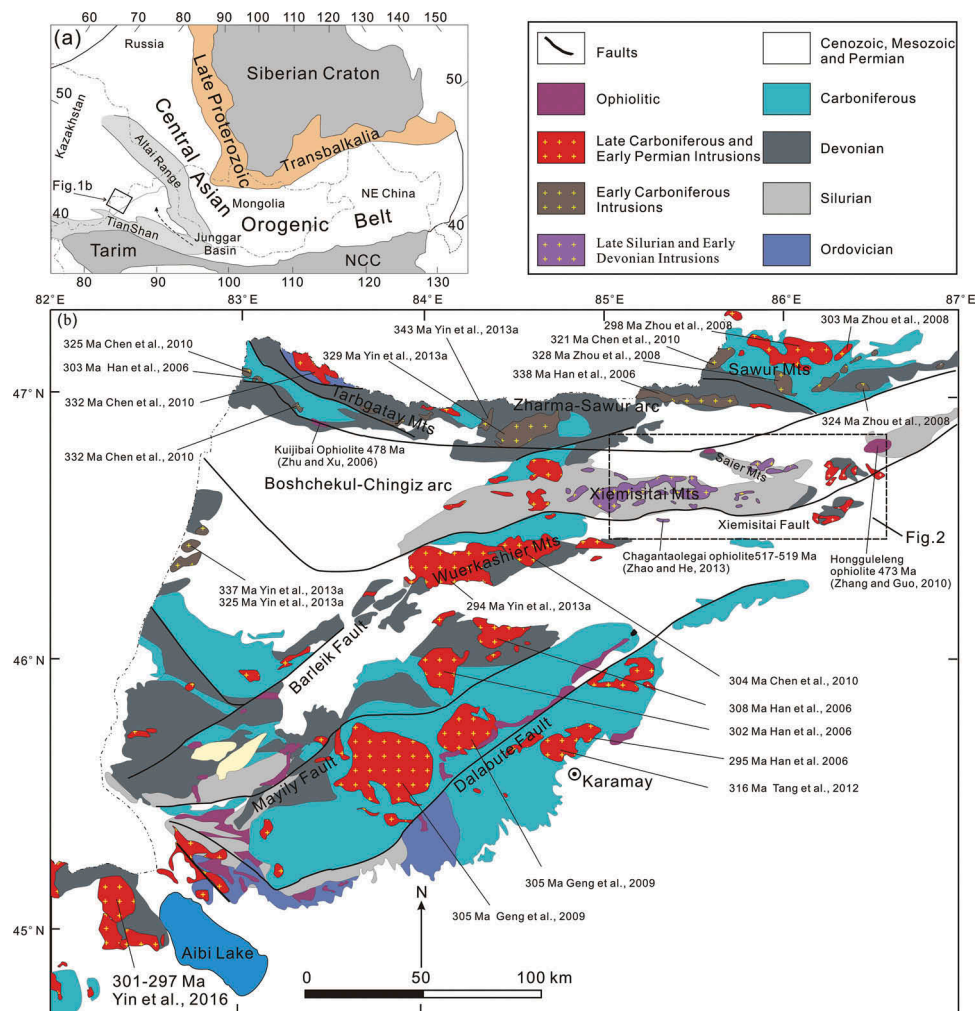
Figure 1. (a) Simplified tectonic divisions of the Central Asian Orogenic Belt (after Jahn *et al.* 2000). (b) Simplified geological map of the West Junggar (modified after Yin *et al.* 2017). Reproduced by permission of Wen Chen.

Zhao and He 2013). Therefore, its Palaeozoic tectonic history is potentially correlated with that of the Kazakhstan orocline and more detailed studies are necessary.

The West Junggar is primarily composed of Palaeozoic intrusive and volcanic rocks. Volcanic rocks in this area mainly consist of Silurian to Carboniferous andesitic basalt, andesite, dacite, felsic tuff, and tuffite (Geng *et al.* 2011; Shen *et al.* 2012; Yang *et al.* 2014). Recently, late Silurian–early Devonian magmatism has been distinguished (Table 1; Chen *et al.* 2010; Chen *et al.* 2015; Yin *et al.* 2017). Despite the many studies that have been carried out in the area, the geodynamic setting of West Junggar remains controversial. Based on the occurrence of the Late Silurian–Early Devonian I-type and A-type granites and their undeformed and alkali-enriched characteristics, these granitic plutons in northern West Junggar were previously interpreted as granites formed in a post-collisional setting (Chen *et al.* 2010, 2015). The middle Palaeozoic Xiemisitai volcanic

rocks consist mainly of andesite, rhyolite, and their pyroclastic equivalents (Shen *et al.* 2012). All of these rocks show typical arc-like geochemical characteristics (e.g. enrichment of large ion lithophile elements (LILEs) and strong negative anomalies of Ta, Nb, P, and Ti). Shen *et al.* (2012) and Yang *et al.* (2014) considered that the middle Palaeozoic volcanic rocks were likely generated in a normal arc-related setting. Most recently, a Devonian mantle plume model has been invoked to account for the alkaline basalts from the Karamay ophiolitic mélange, because the basalts show typical Ocean-Island Basalt (OIB) affinity (Yang *et al.* 2013, 2015). In contrast with the extensive distribution of granitic magmatism and volcanic rocks in the West Junggar, mafic dikes are relatively sporadic and sparse, mainly derived from partial melting of the lithospheric mantle or asthenosphere during the lithospheric-scale extension (e.g. Gudmunsson 1995). Previous works mainly focused on the Early Carboniferous (Yin *et al.* 2015a), and the late Carboniferous–middle Permian

Table 1. Summary of sample localities and ages of the intrusions in the Xiemisitai–Saier Mountain.

Samples	Locality	GPS position	Lithology	Age (Ma)	Method	Data sources
WJ1122	Xiemisitai Mts	46°41′36″N, 85°32′20.2″E	Gabbro	420 ± 3	LA-ICP-MS	Yin et al. 2017
WJ1125	Xiemisitai Mts	46°42′38.3″N, 85°30′20.0″E	K-feldspar granite	420 ± 1	LA-ICP-MS	
WJ1126	Xiemisitai Mts	46°42′28.7″N, 85°27′34.9″E	Syenitic granite	418 ± 2	LA-ICP-MS	
WJ1128	Xiemisitai Mts	46°34′44.3″N, 85°28′30.0″E	Rhyolite	419 ± 2	LA-ICP-MS	
WJ1132	Xiemisitai Mts	46°39′32.4″N, 85°36′60″E	Granodiorite	420 ± 2	LA-ICP-MS	
WJ1311	Xiemisitai Mts	46°42′23.9″N, 85°06′54.7″E	Granodiorite	419 ± 2	LA-ICP-MS	
WJ1312	Xiemisitai Mts	46°42′56.1″N, 85°19′36.6″E	K-feldspar granite	420 ± 2	LA-ICP-MS	
WJ1136	Saier Mts	46°45′43″N, 85°53′18.5″E	Syenitic granite	407 ± 3	LA-ICP-MS	
XMST08	Xiemisitai Mts	46°42′39″N, 85°31′07″E	K-feldspar granite	419 ± 2	SHRIMP II	Chen et al. 2010
XMST14	Xiemisitai Mts	46°42′39″N, 85°31′07″E	Diorite	422 ± 2	SHRIMP II	
XMST02	Xiemisitai Mts	46°42′39″N, 85°31′07″E	Alkaline granite	417 ± 4	SHRIMP II	
XMST01	Xiemisitai Mts	46°35′05″N, 85°30′25″E	K-feldspar granite	420 ± 4	SHRIMP II	
XMST03	Xiemisitai Mts	46°34′44″N, 85°29′09″E	Rhyolite-Porphyry	420 ± 5	SHRIMP II	
HZ	Xiemisitai Mts	46°36′42″N, 85°52′28″E	Rhyolite-Porphyry	414 ± 5	SHRIMP II	
HLSL	Saier Mts	46°44′16″N, 85°48′44″E	Felsite	405 ± 4	LA-ICP-MS	
CGKL	Saier Mts	46°45′56″N, 85°53′39″E	K-feldspar granite	410 ± 3	SHRIMP II	
HBK	Saier Mts	46°46′32″N, 85°40′42″E	K-feldspar granite	417 ± 5	SHRIMP II	
QS-1	Xiemisitai Mts		Quartz syenite	418 ± 5	LA-ICP-MS	Chen et al. 2015
D-1	Xiemisitai Mts		Diorite	424 ± 5	LA-ICP-MS	
MG-1	Xiemisitai Mts		Monzogranite	418 ± 5	LA-ICP-MS	
S-1	Xiemisitai Mts		Syenite	392 ± 6	LA-ICP-MS	
HG-1	Xiemisitai Mts		Hornblende gabbro	422 ± 5	LA-ICP-MS	
14XMST02	Xiemisitai Mts	46°42′18.1″N, 85°30′58.5″E	Mafic dike	406 ± 5	^{40}Ar-^{39}Ar	This study
WJ1314	Xiemisitai Mts	46°38′41.2″N, 85°47′36.1″E	Monzogranite	414 ± 3	LA-ICP-MS	

mafic-intermediate dikes (Qi 1993; Li et al. 2004; Xu et al. 2008; Yin et al. 2010, 2013b, 2015b; Ma et al. 2012; Tang et al. 2012). However, the early Devonian mafic dike–granite associations have not been systematically studied, and their age, petrogenesis, and geodynamic processes remain to be unravelled. In this article, we present LA-ICP-MS zircon U–Pb and hornblende ^{40}Ar-^{39}Ar ages and major-element and trace-element data for the Xiemisitai mafic dike–granite association in the northern West Junggar. The results will not only constrain their ages and petrogenesis, but also improve our understanding of the geodynamic evolution in the West Junggar and adjacent areas during the middle Palaeozoic.

2. Geologic background and samples

The West Junggar is divided into northern and southern parts by the Xiemisitai Fault (Figure 1(b); Xu et al. 2012). The northern West Junggar is mainly characterized by two E–W-trending faults (Xiemisitai Fault and Sawur Fault) (Figure 1(b); Chen et al. 2010). Several ophiolites [i.e. Kujibai (478 Ma), Honggguleleng (473 Ma), Chagantaolegai (517–519 Ma)] have been reported along the Xiemisitai and Sawur Faults in the northern West Junggar, demonstrating a complex accretionary history (Zhu and Xu 2006; Zhang and Guo 2010; Zhao and He 2013). The distribution of magmatic rocks in the northern West Junggar is governed by the Zharma–Sawur and Boshchekul–Chingiz arcs (Figure 1(b)). The Zharma–Sawur arcs are mainly characterized by

subduction-related Devonian–early Carboniferous volcanic rocks (Shen et al. 2008), Carboniferous I-type granitoids (Zhou et al. 2008; Chen et al. 2010; Yin et al. 2013a), and early Permian A-type granitoids (Zhou et al. 2008). The Boshchekul–Chingiz arcs, however, consist of early Silurian to early Carboniferous calc-alkaline volcanic rocks (Shen et al. 2012; Yang et al. 2014), late Silurian–early Devonian A-type granites and associated mafic-intermediate to felsic intrusions and volcanic to sub-volcanic rocks (Table 1; Chen et al. 2010; Chen et al. 2015; Meng et al. 2010; Shen et al. 2012; Wang et al. 2014; Yin et al. 2017), and late Carboniferous–early Permian granitoids (Yin et al. 2013a). Currently, Ar–Ar dating and geochemical studies are absent for the mafic dikes in the Xiemisitai Mountains. They dip steeply and occur mainly in the E–W (270°) and NW-W (290°) trends (Figure 3(a,b)). They range in width from 0.5 to 2m, and in length from 100 to 1000 m. The mafic dikes intruded mainly the late Silurian–early Devonian granitic intrusions (Figures 2 and 3(a,b)). In this study, 15 samples were collected from two dikes and one pluton in the Xiemisitai Mountains (Figures 2 and 3(c–e)). The mafic dikes are generally undeformed and most underwent slight alteration (Figure 3(c)). The mafic dike WJ1310 has a porphyritic texture and a massive structure; the phenocrysts mainly consist of plagioclase and hornblende (Figure 3(f–g)). The groundmass is composed of plagioclase (60 vol.%), hornblende (15 vol.%), biotite (5 vol.%), and minor amount of quartz (Figure 3(f–g)). The mafic dike
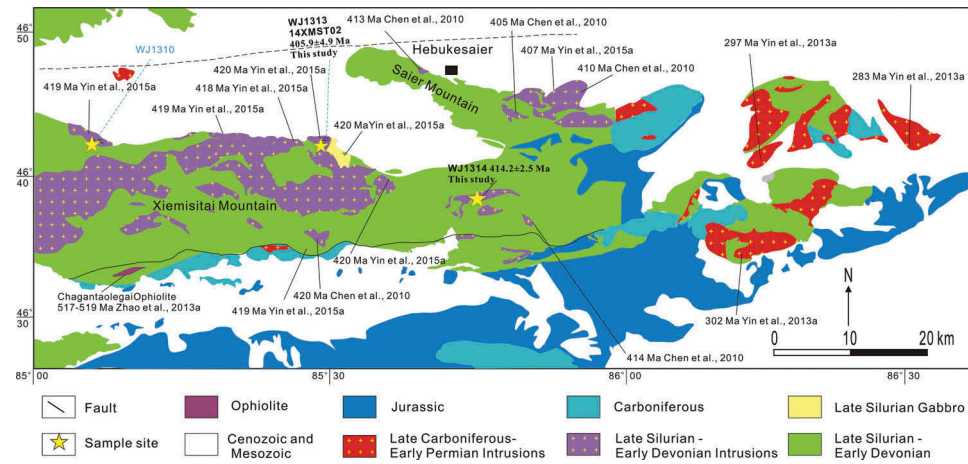
Figure 2. Geological map of the Xiemisitai and Saier mountains in the northern West Junggar (modified after Yin *et al*. 2017). Reproduced by permission of Wen Chen.
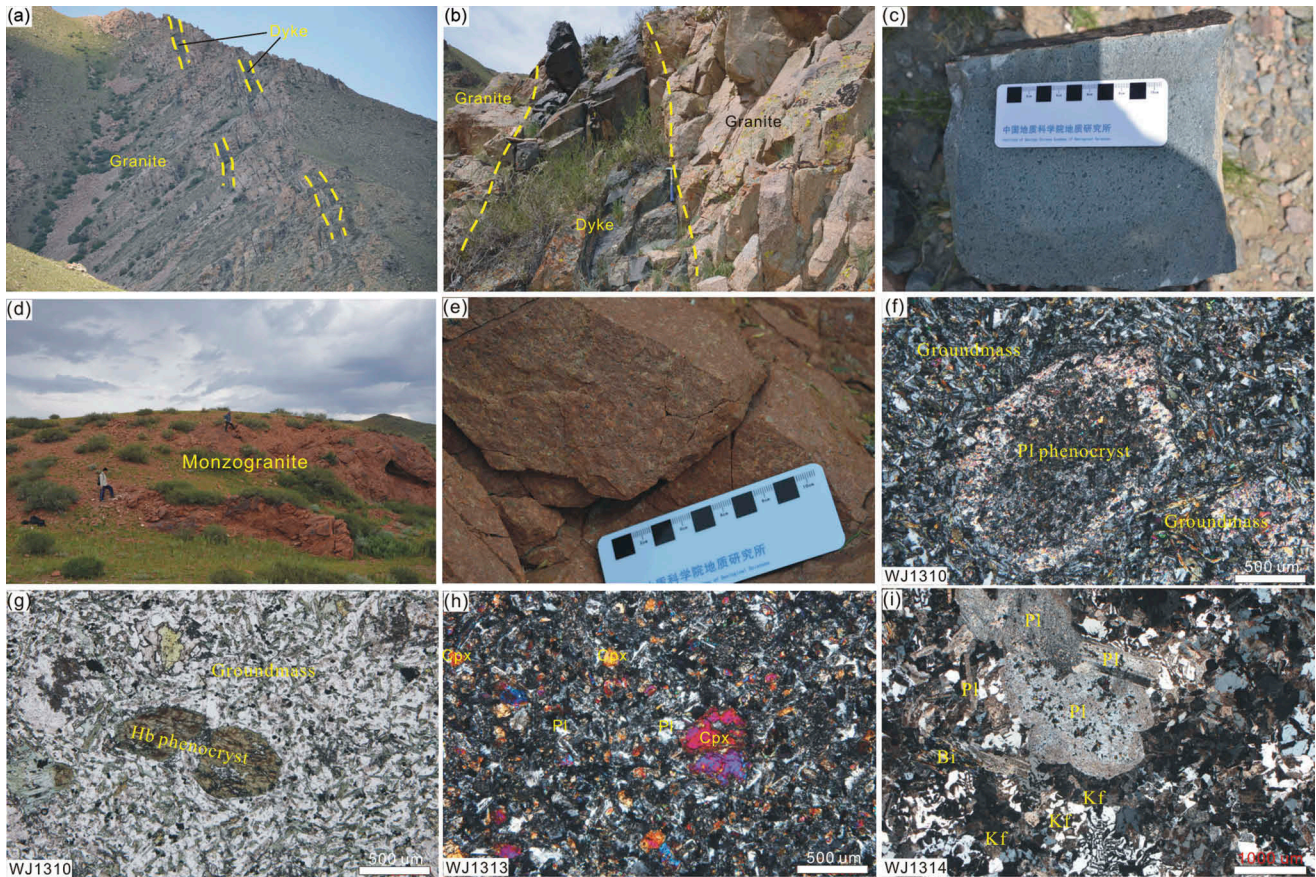

Figure 3. Field and microscopic photographs of the Xiemisitai dikes and monzogranites in the northern West Junggar. (a–b) The granite intruded by the mafic dike; (c) hand specimen of the mafic dike; (d–e) field outcrop and hand specimen of the monzogranites; (f) mineral compositions and texture of the monzogranites; (g–i) mineral compositions and texture of the mafic dike. Kf, K-feldspar; Bi, biotite, Cpx, clinopyroxene; Pl, plagioclase; Hb, hornblende.

WJ1313 is also porphyritic in texture, with clinopyroxene (5 vol.%) and plagioclase (1–5 vol.%) phenocrysts up to 1 mm long in a groundmass of fine-grained to microcrystalline plagioclase (55 vol.%), clinopyroxene (30 vol.%), biotite (5 vol.%), and minor quartz (Figure 3(h)). The monzogranite in the Xiemisitai Mountain contains phenocrysts up to 3.7 mm, which were mainly composed of K-feldspar

(35 vol.%). The groundmass consists of plagioclase (15 vol.%), K-feldspar (25 vol.%), quartz (20 vol.%), mafic minerals (5 vol.%), and accessories (Figure 3(f)).

3. Analytical methods

3.1. Major- and trace-element analyses

Major-element compositions were obtained by X-ray fluorescence spectrometry (XRF) on fused glass beads using a Rigaku 100e spectrometer at the Guangzhou Institute of Geochemistry, Chinese Academy of Sciences (GIGCAS). Details of the procedures are described by Yuan *et al*. (2010). Abundances of trace elements, including rare earth elements (REEs), were determined using a Perkin-Elmer ELAN 6000 inductively coupled plasma source mass spectrometer (ICP-MS) at GIGCAS, following the procedures described by Li *et al*. (2002). Selected relatively fresh rocks were first split into small chips and ultrasonically cleaned in distilled water, then powdered after drying and handpicking to remove visible contamination. The powdered samples (50 mg) were dissolved in screw-top Teflon beakers using an HF + HNO_3 mixture for 7 days at ~100□. An internal standard solution containing the single element Rh was used to monitor drift in mass response during counting. USGS standard BCR-1 was used to calibrate the elemental concentrations of the measured samples. Precision for REE and other incompatible elements is estimated to be better than 5% from the international USGS reference samples BIR-1 and laboratory standard (ROA-1). In-run analytical precision for Nd is less than 2.5% RSD (relative standard deviation). The Sm/Nd ratios measured by ICP-MS are within 2% uncertainty, and the calculation of $\varepsilon_{Nd}(t)$ values for the samples of the present study using these Sm/Nd ratios will result in uncertainties of less than 0.25 units, which are negligible for petrogenetic discussion.

3.2. ^{40}Ar-^{39}Ar geochronology

^{40}Ar-^{39}Ar dating was performed at the Laboratory of Isotope Thermochronology (LIT), Institute of Geology, Chinese Academy of Geological Sciences (CAGS) (Beijing, China). Purified argon was released into the Helix MC Mass Spectrometer for argon isotope analysis. The monitor (ZBH-25) used as an internal standard is Fangshan biotite with an age of 132.7 ± 1.2 Ma and a potassium (K) content of 7.579 ± 0.030 wt.% (Wang 1983). The plateau ages (quoted at±2σ) and isochron diagrams were calculated with ISOPLOT (Ludwig 2001). See Chen *et al*. (2006) and Zhang *et al*. (2006) for a detailed description of the procedure.

3.3. Zircon U–Pb geochronology

Zircon U–Pb isotopic compositions were analysed using an Agilent 7700x ICP-MS equipped with an ArF excimer laser system (GeoLas Pro, 193 nm wavelength) in the Chinese Academy of Science Key Laboratory of Crust–Mantle Materials and Environments, University of Science and Technology of China (USTC). Standards 91500, Mon-1, GJ-1, and NIST610 were used during the analyses. The analyses were carried out with a pulse rate of 10 Hz and a beam energy of 10 J/cm^2 with a spot diameter of 44 µm. ^{29}Si was used as internal standards for zircon. Certified glass reference material NIST SRM 610 was used as an external standard, which was analysed twice for every four analyses. The analytical procedures for zircon U–Pb isotopes were similar to those described by Wang *et al*. (2013).

4. Result

4.1. ^{40}Ar–^{39}Ar geochronology

Sample 14XMST02 was selected for hornblende $^{40}Ar/^{39}Ar$ dating. Both samples 14XMST02 and WJ1313 were collected from the same dike and latitude and longitude position. The sample 14XMST02 yields a plateau age of 405.9 ± 4.9 Ma (MSWD = 0.29; 2 error) at heating temperatures between 1030°C and 1140°C (Figure 4(a); Supplementary Table 1), comprising 59.9% of the total ^{39}Ar released. The inverse isochron age (413 ± 12 Ma; Figure 4(b)) is consistent with the plateau age. The hornblende $^{40}Ar/^{39}Ar$ age of the mafic dike is younger than that of the granitic country rocks (420 Ma Yin *et al*. 2017), which is interpreted to represent the crystallization age of the mafic dikes in the Xiemisitai Mountains.

4.2. Zircon U–Pb geochronology

The sample WJ1314 was selected for zircon U–Pb dating. Zircons separated from the sample WJ1314 are light brown or colourless, and have subhedral, stubby to prismatic crystals, generally 50–100 µm in length, with a length to width ratio of around 2.0. The CL images show that most of the grains possess good oscillatory zoning and have no inherited cores with high Th/U ratios (0.68–2.16), indicating a magmatic origin (Belousova *et al*. 2002). Eighteen spots from 18 zircons of a monzogranite (WJ1314) plot on or near the Concordia (Figure 4 (c)), forming a tight cluster with a weighted mean $^{206}Pb/^{238}U$ age of 414.2 ± 2.5 Ma (MSWD = 0.26) (Figure 4(d); Supplementary Table 2). We consider the
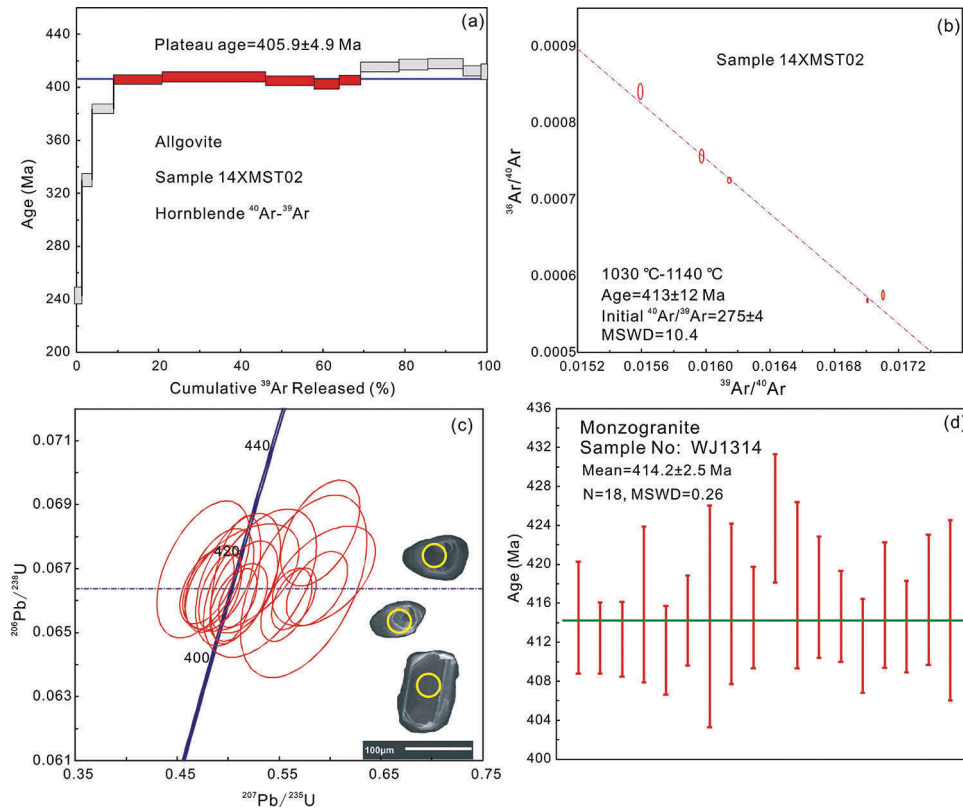
Figure 4. $^{40}Ar/^{39}Ar$ and LA-ICP-MS zircon U–Pb analyses for the Xiemisitai dikes and monzogranites in the Northern West Junggar.

414.2 ± 2.5 Ma age to be the crystallization age of the monzogranite.

4.3. Geochemistry

Chemical compositions of the Xiemisitai mafic dikes are listed in Supplementary Table 3. The mafic dikes have relatively high SiO_2 (51.3–53.9 wt.%) and low MgO (3.88–6.41 wt.%) and TiO_2 (1.01–1.08 wt.%) contents and $Mg^\#$ (46–59) values (Supplementary Table 3). In the total alkalis *versus* silica diagram (Figure 5(a)), all dike samples show sub-alkaline character and plot in the fields of basalt andesite, which is further confirmed in the $Zr/(TiO_2 \times 0.0001)$-Nb/Y diagram (Figure 5(b)). They have very uniform chondrite-normalized REE patterns ($(La/Yb)_N$ = 3.25–3.29) with varying LREE enrichments ($[La/Yb]_N$ = 4.4–8.0) and weak positive or negative Eu anomalies (Eu/Eu* = 0.92–1.03) (Figure 6(a)). In the primitive mantle-normalized variation diagrams, the mafic dikes showed enrichment in highly incompatible elements (e.g. K, Rb, Sr, and Ba) and LREE, but depletion of moderately incompatible elements (e.g. Nb, Ta, and Ti) and HREE (Figure 6(b)). In addition, trace-element distribution patterns of the mafic dikes are different from those of arc volcanics (Figure 6(b)). The monzogranites have high SiO_2 (70.6–

71.1 wt.%), K_2O (4.15–4.32 wt.%), and $Na_2O + K_2O$ (8.82–9.04 wt.%) contents (Supplementary Table 3) and are weakly peraluminous (A/CNK = 1.02–1.07) (Figure 5(c)). On the Quartz, Alkali feldspar, Plagioclase, Feldspathoid (QAPF) modal diagram, all samples plot in the alkali-feldspar-granite area (Figure 5(d)). They have relatively low MgO (0.53–0.57 wt.%), TiO_2 (0.40–0.43 wt.%), Cr (3.79–10.2 wt.%), and Ni (1.20–6.49 wt.%) concentrations (Supplementary Table 3). The monzogranites are enriched in LREEs relative to HREEs with $(La/Yb)_N$ ratios of 8.48–9.69 (Figure 6(a)). They have obvious negative Eu anomalies, with Eu/Eu* values of 0.72–0.79. On primitive mantle-normalized trace element diagrams, they are enriched in LILEs, such as Rb, Ba, Th, and U and depleted in HFSEs with negative Nb, Ta, P, and Ti anomalies (Figure 6(b)), consistent with the geochemical characteristics of subduction-related magmas.

5. Discussion

5.1. Mantle source nature and petrogenesis of the mafic dikes

The Xiemisitai mafic dikes were characterized by low $Mg^\#$ (46–59) and low Cr (11.3–197 ppm) and Ni (19.9–102 ppm) abundances (Supplementary Table 3) compared with mantle-derived primary melts [(Ni>400 ppm,
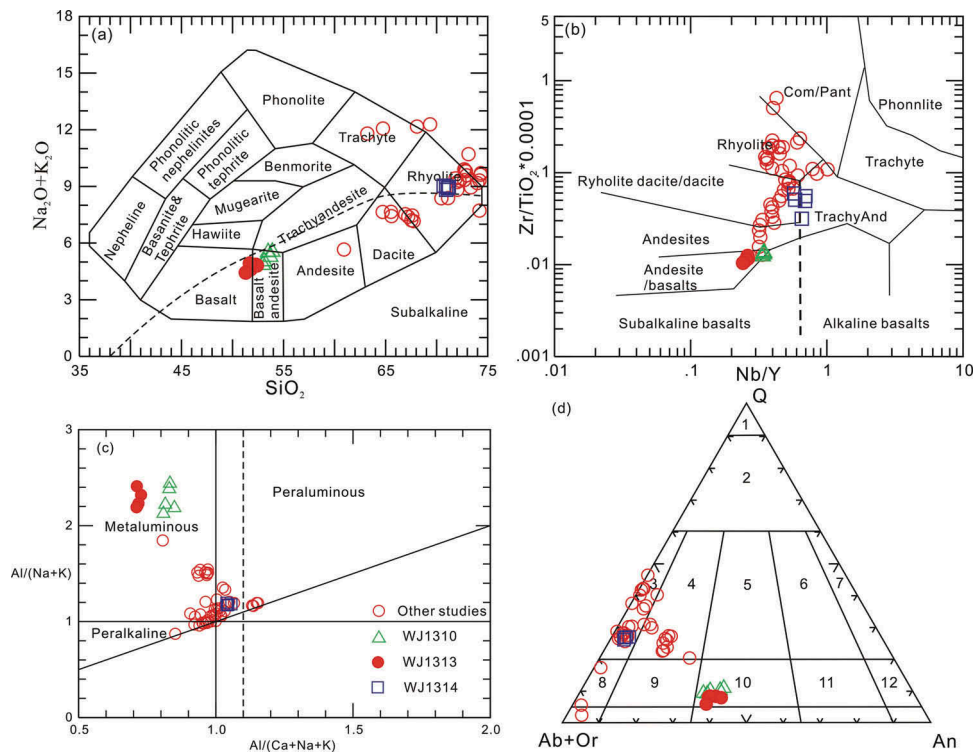
Figure 5. Geochemical classification diagrams for the Xiemisitai dikes and monzogranites in the Northern West Junggar. (a) Total alkalis *versus* silica diagram (after Le Bas *et al*. 1986); (b) Zr/(TiO$_2$ × 0.0001)–Nb/Y diagram (after Winchester and Floyd 1977); (c) A/CNK *versus* A/NK diagram (Maniar and Piccoli 1989); (d) QAPF diagram (Streckeisen 1978; Le Maitre 2002). 1, quartzolite; 2, quartz-rich granitioids; 3, alkali feldspar granite; 4, syeno-granite; 5, monzo-granite; 6, granodiorite; 7, tonalite; 8, quartz alkali feldspar syenite; 9, quartz syenite; 10, quartz monzonite; 11, quartz monzodiorite, quartz-monzogabbro; 12, quartz diorite, quartz-gabbro, quartz-anorthosite. The data of other studies is from Chen *et al*. (2015) and Yin *et al*. (2017). Reproduced by permission of Wen Chen.

Cr>1000 ppm (Wilson 1989), and Mg$^{\#}$ = 73–81 (Sharma 1997)], suggesting that the Xiemisitai mafic dikes have experienced significant fractional crystallization. When magmas rise from mantle sources to the continental crust, crustal contamination could have significantly changed their incompatible elements compositions as shown by their elevated Th/La, (La/Ta)$_N$, and (Th/Ta)$_N$ ratios. However, we noticed that the Nb/La ratios in these samples remain virtually unchanged irrespective of the MgO contents. This suggests the Nb–Ta deficits in the Xiemisitai mafic dikes were inherited from the source, rather than from crustal contamination. The Xiemisitai mafic dikes display negative Nb–Ta–Ti anomalies, enrichment of LREEs and LILEs, and depletion of HREEs and HFSEs. However, as discussed above, crustal contamination did not play a major role during the formation of the Xiemisitai mafic dikes. Therefore, the enrichment of the LILEs and the negative Nb–Ta anomalies from the Xiemisitai mafic dikes suggest a subduction zone component. The presence of residual hydrous mineral phases (e.g. amphibole) indicates that the Xiemisitai mafic dikes are likely derived from a lithospheric mantle, because these minerals are not

stable in the hot and anhydrous convecting asthenosphere, but are stable under the conditions found in the lithospheric mantle (Foley 1992; Class and Goldstein 1997). Therefore, the Xiemisitai mafic dikes likely represent melts derived from a lithospheric mantle metasomatized by subducted slab-derived fluids.

The nature of the mantle source and the extent of melting could be distinguished by REE fractionation patterns (George *et al*. 2003). Figure 7(a) displays the [Sm/Yb]$_N$ *versus* [La/Sm]$_N$ ratios for the Xiemisitai mafic dikes, along with the batch equilibrium melting trends for different proportions of clinopyroxene and garnet left in the solid residue, and for different degrees of partial melting (D'Orazio *et al*. 2001). Yb is compatible in garnet; La and Sm are, however, incompatible, and hence La/Sm and Sm/Yb will be intensively fractionated when the melting degree is low. La/Sm, by contrast, is only slightly fractionated and Sm/Yb is almost unfractionated during melting in the spinel stability field. It is noted that the Xiemisitai mafic dikes are consistent with melting trends with little to no garnet (Cpx: Grt = 6:1) in their source, suggesting a 1–2% degrees of batch melting. The La/Yb *versus* Tb/Yb plot (Figure 7(b)) further confirms the above-mentioned result and indicates
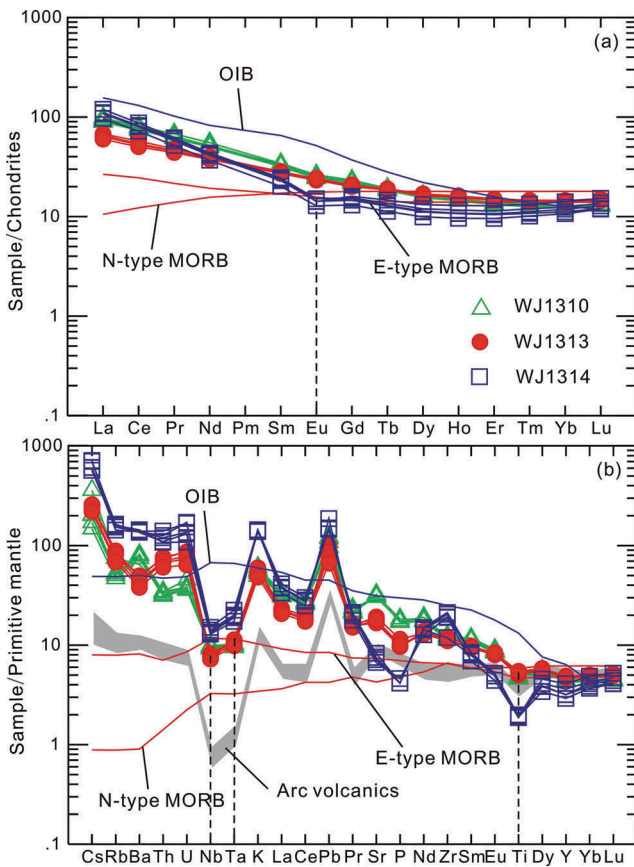
Figure 6. Chondrite-normalized rare earth element patterns and Primitive Mantle (PM)-normalized trace element diagrams for the Xiemisitai dikes and monzogranites in the northern West Junggar. The chondrite, PM, OIB, N-MORB, and E-MORB data are from Sun and McDonough (1989). Arc volcanics data are from Luhr and Haldar (2006). Reproduced by permission of Wen Chen.

Figure 7. (a) Sm/Yb *versus* La/Sm (D' Orazio *et al*. 2001) and Tb/Yb *versus* La/Yb (George and Rogers 2002) diagrams for the Xiemisitai dikes in the northern West Junggar.

the presence of less than 1% residual garnet in the source region for Xiemisitai mafic dikes. The degree of partial melting was 1–2% (Figure 7(b)) according to calculations of REE fractionation. Therefore, it can be inferred that the Xiemisitai mafic dikes were generated at a correspondingly shallow depth, mostly within the spinel stability field. If the concept of the melting column (Langmuir *et al*. 1992) is viable and the depth of the spinel to garnet transition at the peridotite solidus is assumed to be ~75–80 km (McKenzie and O' Nions 1991), then the result implies that the decompressing asthenosphere rose to a relatively shallow level (<80 km).

5.2 Petrogenesis of the monzogranites

The monzogranites have low A/CNK ratio<1.1 (Figure 5(c)) and medium to high K_2O contents and calc-alkaline affinity, consistent with the geochemical features of I-type granites (Chappell and White 1992; Chappell 1999). The monzogranites were unlikely generated by direct melting of a mantle
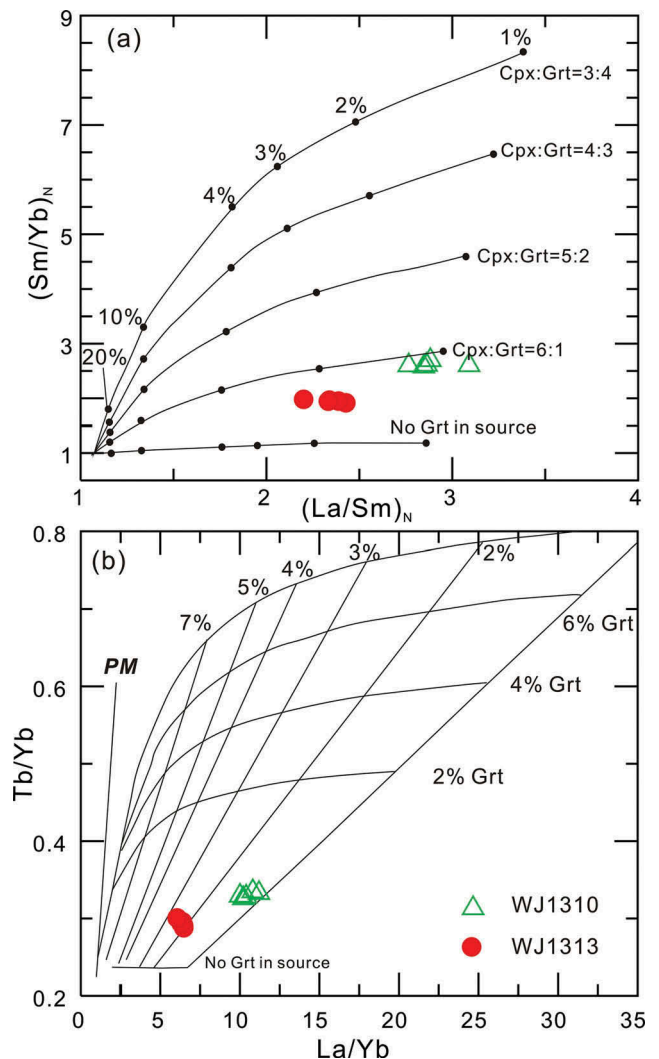
source, given that their silica contents are as high as 70 wt. % and their Mg# are as low as 40. Experimental results can provide insights into the melt compositions produced from different sources and the P–T conditions of melt generation. The monzogranites have intermediate Na_2O and medium to high K_2O contents at high silica contents, identical to the compositions of melts produced by partial melting of the medium to high K basaltic rocks (Figure 8(a, b); Beard and Lofgren 1991). The monzogranites have comparable trace-element patterns, characterized by relative enrichments of LREE and the depletion of HFSE (e.g. Nb, Ta, and Ti), consistent with the geochemical characteristics of subduction-related magmas (Figure 6(a,b)). Given that the Xiemisitai A-type granites and I-type granites have depleted Nd–Sr–Hf isotope compositions in the same area (Chen *et al*. 2015; Yin *et al*. 2017), it suggests that the contemporaneous Xiemisitai monzogranites were likely
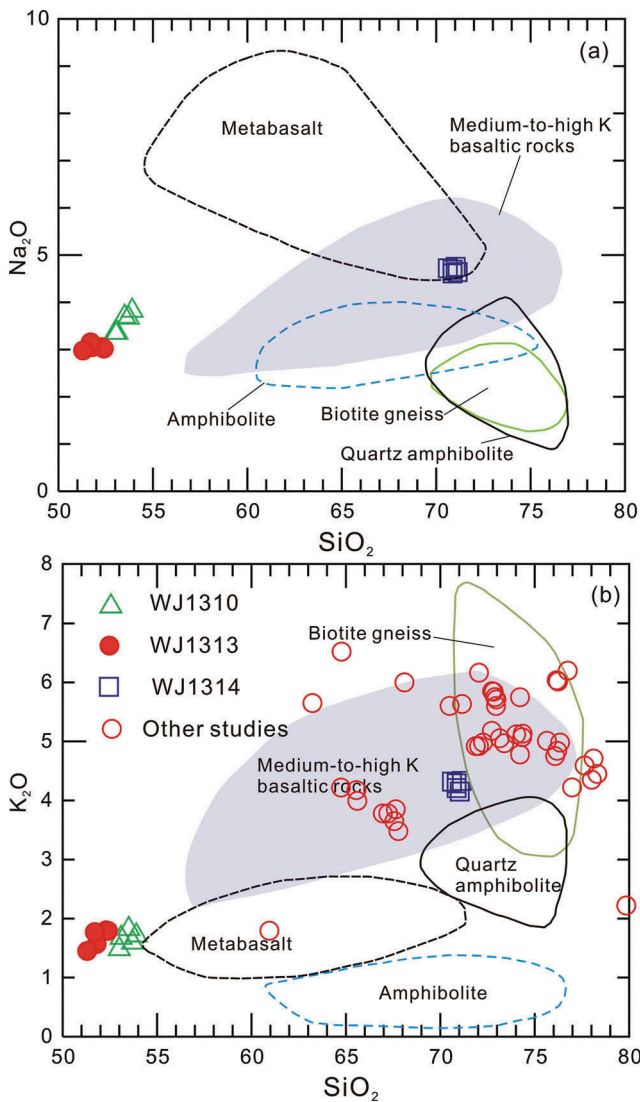
Figure 8. SiO$_2$ *versus* Na$_2$O and K$_2$O for the Xiemisitai monzogranites compared with the experimental melts (a–b). Experimental melts are from Beard and Lofgren (1991) (amphibolites; 1, 3, 6, 9 kb; 800–1000□), Rapp and Watson (1995) (metabasalt; 8–32 kb; 1000–1125□), Patiño Douce and Beard (1995) (quartz amphibolites; 3–15 kb; 850–930□); Patiño Douce and Beard (1995) (biotite gneiss; 3–15 kb; 850–930□); and Sisson *et al*. (2005) (medium to high K basaltic rocks; 700 Mpa; 825–975□). The data of other studies are from Chen *et al*. (2015) and Yin *et al*. (2017). Reproduced by permission of Wen Chen.

derived from the same origin with them. Therefore, the Xiemisitai monzogranites were also probably generated by the partial melt of the juvenile mid-lower crust.

5.3 Implications for tectonic evolution

The late Silurian–early Devonian igneous rocks are widespread in the Xiemisitai Mountains of West Junggar and mostly consist of adakitic granodiorite,

A-type and I-type granites, and mafic dikes (Chen *et al*. 2010, 2015; Yin *et al*. 2017; this study). As discussed above, the mafic dikes would be generated by the partial melting of a lithospheric mantle at relatively shallow depths (<80 km). The adakitic granodiorites and A-type granites are also regarded as products of high-temperature magmatism (Yin *et al*. 2017). The coexistence of adakitic granodiorites, A-type granites, and mafic dikes in the Xiemisitai Mountains of the northern West Junggar indicates a high-temperature extensional regime during the late Silurian–early Devonian. Different types of dynamic mechanisms can be proposed to account for the fact that a high-temperature regime, thin lithosphere, and magmatic 'flare-up' were all occurring in the Xiemisitai Mountains of the northern West Junggar during the late Silurian–early Devonian (Figure 9), that is, (1) delamination in a post-collisional setting (Chen *et al*. 2010, 2015); (2) mantle plume ascent (Yang *et al*. 2013, 2015); or (3) ridge subduction or slab rollback (Yin *et al*. 2017).

The crustal delamination model requires previous crustal thickening to produce a dense eclogitic crustal root. The lower crust is generally much drier than the subducting oceanic crust. However, the mafic dikes include hydrous mineral phases with enrichment of LREEs and LILEs and depletion of HREEs and HFSEs (Figure 6(a,b)), which imply a fluid-assisted metasomatized source. All mafic dikes fall into the area of arc-basalts on an Hf/3-Th-Ta tectonic discriminant diagram (Figure 10(a)). The Xiemisitai mafic dikes and monzogranites also all plot in the volcanic arc field on the Yb–Ta tectonic discrimination diagram (Figure 10(b)), suggesting that the mafic dike–granite association formed in a subduction-related setting. Thus, the
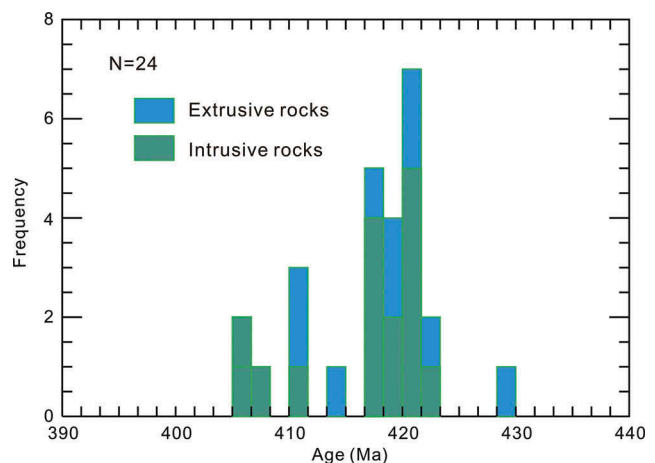

Figure 9. Histogram of dates interpreted as a magmatic 'flare-up' in the northern West Junggar region during 429–405 Ma. Age data are from Yin *et al*. (2017) and references therein and this study. Reproduced by permission of Wen Chen.
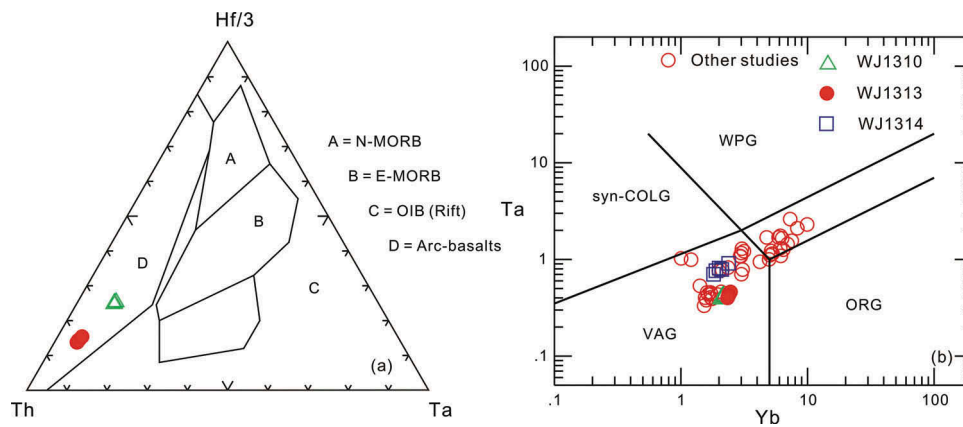
Figure 10. (a) The Xiemisitai dikes on the Th-Hf/3-Ta discrimination diagram of Wood (1980). (b) Tectonic discrimination plot for the Xiemisitai dikes and monzogranites (Pearce *et al*. 1984). The data of other studies are from Chen *et al*. (2015) and Yin *et al*. (2017). Reproduced by permission of Wen Chen.

mafic dike–granite association cannot be readily explained by the delamination model. In addition, the delamination model in a post-collisional setting is also not supported by the palaeomagnetic, palaeogeographic, and sedimentary evidence and as discussed in detail in Yin *et al*. (2017).

Yang *et al*. (2013) and Yang *et al*. (2015) suggested that the middle Devonian alkaline basalts from the Karamay ophiolitic mélange in the West Junggar can be correlated to a mantle plume-related magmatism within the Palaeo-Asian Ocean. The basalts are alkaline and characterized by LILE and LREE enrichment, HREE depletion, very weak or no Eu anomalies (Eu/Eu* = 0.9–1.0), and no obvious Nb, Ta, and Ti negative anomalies, suggesting a typical OIB affinity (Yang *et al*. 2013). Our study indicates that mafic dikes, however, are dissimilar to OIB (Figure 6(a,b)) and were probably generated by a metasomatized lithospheric mantle at relatively shallow depths (<80 km), mostly within the spinel stability field. In addition, the middle Silurian–early Devonian volcanic rocks in the Xiemisitai Mountains are mainly calc-alkaline and intermediate-felsic, with minor amounts of mafic rocks, and show enrichment in LILEs and depletion in HFSEs, akin to typical island arc-type volcanic rocks (Shen *et al*. 2012; Yang *et al*. 2014). More importantly, the age of the Xiemisitai mafic dikes (405.9 ± 4.9 Ma, this study) is older than the age of the Karamay alkaline basalt (395–387 Ma). Thus, this suggests that the formation of the Xiemisitai mafic dikes was not related to a Devonian mantle plume.

Prior to 425 Ma, the Xiemisitai area could be a normal subduction system because there only occurred calc-alkaline volcanic rocks (Figure 11(a); Yang *et al*. 2014). During late Silurian–early

Devonian, many adakitic granodiorites and A-type granites occurred in the Xiemisitai–Saier Mountains. In our previous studies, we have systematically discussed the petrogenesis of this high-temperature magmatism from Xiemisitai Mountains in the northern West Junggar (Yin *et al*. 2017). The adakitic granodiorites were likely generated by the partial melting of the mafic lower crust, leaving an amphibole and garnet residue. The A-type and I-type granites were likely formed by partial melting of the Xiemisitai mid-lower crust. Although both ridge subduction and slab rollback could provide a high-temperature extensional setting, we are inclined to favour the slab rollback model as a possible mechanism during the late Silurian–early Devonian time in the northern West Junggar as discussed in detail in Yin *et al*. (2017). Consequently, during the process of slab rollback, the upwelling asthenospheric mantle would have possibly provided enough heat for the partial melting of the overlying lithospheric mantle that had previously been metasomatized by subducted slab-derived fluids. Accordingly, the Xiemisitai mafic dikes were most probably generated by partial melting of the metasomatized lithospheric mantle at relatively shallow depths, mostly within the spinel stability field (Figure 11(b)). The monzogranites were likely formed by partial melting of the Xiemisitai mid-lower crust.

6. Conclusion

(1) Hornblende $^{40}Ar/^{39}Ar$ age of the Xiemisitai mafic dikes from the northern West Junggar indicate that they were emplaced at 405.9 ± 4.9 Ma.
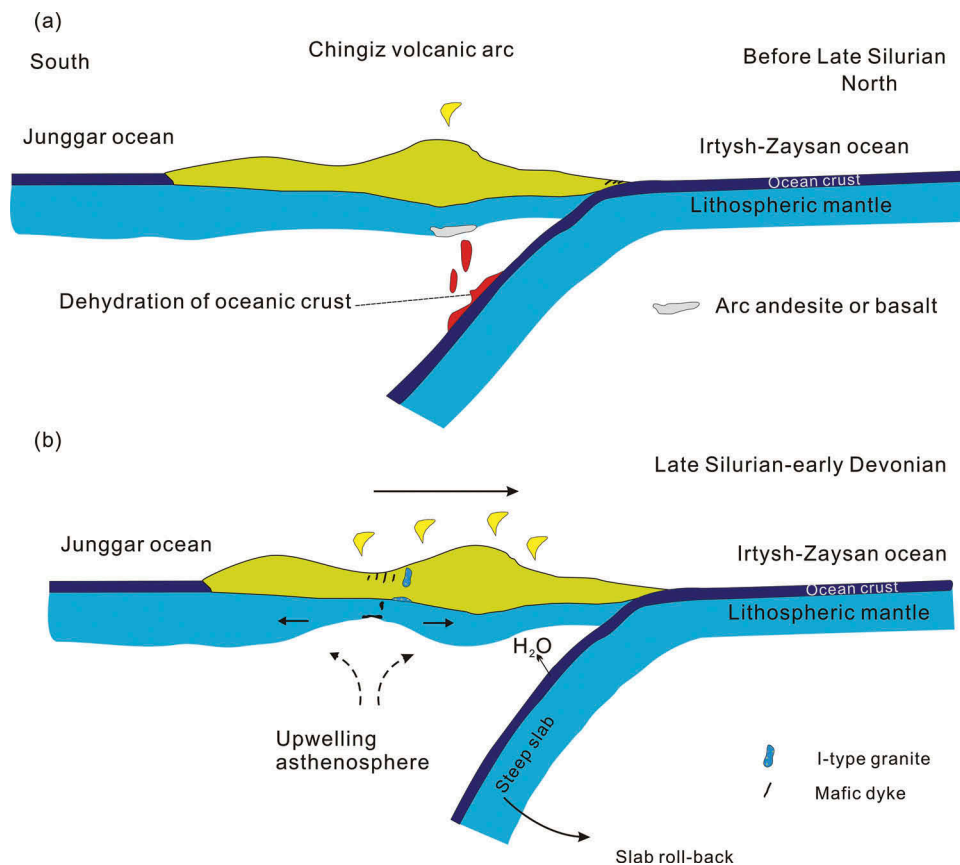(2) The Xiemisitai monzogranites from the northern West Junggar were emplaced at ~414 Ma and

Figure 11. Suggested tectonic model for the Xiemisitai–Saier Mountain in the Middle Palaeozoic (modified after Yin *et al*. (2017)). Reproduced by permission of Wen Chen.

display I-type affinity. They were probably generated by partial melt of the juvenile mid-lower crust.

(3) The Xiemisitai mafic dikes were likely derived by partial melting of a lithospheric mantle metasomatized by subducted slab-derived fluids at a relatively shallow level (<80 km).

(4) The Xiemisitai mafic dike–granite association was possibly triggered by asthenospheric upwelling as a result of the rollback of the subducted Irtysh–Zaysan oceanic lithosphere.

Acknowledgements

Disclosure statement

No potential conflict of interest was reported by the authors.

Funding

References

Beard, J.S., and Lofgren, G.E., 1991, Dehydration melting and water-saturated melting of basaltic and andesitic greenstones and amphibolites at 1, 3, and 6, 9 kb: Journal of Petrology, v. 32, p. 365–401. doi:10.1093/petrology/32.2.365

Belousova, E.A., Griffin, W.L., Suzanne, Y.O.R., and Fisher, N.I., 2002, Igneous zircon: Trace element composition as an indicator of source rock type: Contributions to Mineralogy and Petrology. v. 143, no. 5, p. 602–622. doi:10.1007/s00410-002-0364-7

Chappell, B.W., 1999, Aluminium saturation in I- and S-type granites and the characterization of fractionated haplogranites: Lithos, v. 46, p. 535–551. doi:10.1016/S0024-4937(98)00086-3

Chappell, B.W., and White, A.J.R., 1992, I- and S-type granites in the Lachlan Fold Belt: Transactions of the Royal Society of Edinburgh: Earth Sciences, v. 83, p. 1–26. doi:10.1017/S0263593300007720

Chen, J.F., Han, B.F., Ji, J.Q., Zhang, L., Xu, Z., He, G.Q., and Wang, T., 2010, Zircon U–Pb ages and tectonic implications of Paleozoic plutons in northern West Junggar, North Xinjiang, China: Lithos, v. 115, p. 137–152. doi:10.1016/j.lithos.2009.11.014

Chen, J.F., Han, B.F., Zhang, L., Xu, Z., Liu, J.L., Qu, W.J., Li, C., Yang, J.H., and Yang, Y.H., 2015, Middle Paleozoic initial amalgamation and crustal growth in the West Junggar (NW China): Constraints from geochronology, geochemistry and Sr–Nd–Hf-Os isotopes of calc-alkaline and alkaline intrusions in the Xiemisitai–Saier Mountains: Journal of Asian Earth Sciences, v. 113, p. 90–109. doi:10.1016/j.jseaes.2014.11.028

Chen, W., Zhang, Y., Zhang, Y.Q., Jin, G.S., and Wang, Q.L., 2006, Late Cenozoic episodic uplifting in southeastern part of the Tibetan plateau–evidence from Ar–Ar thermochronology: Acta Petrologica Sinica, v. 22, no. 4, 867–872. [in Chinese with English abstract.]

Class, C., and Goldstein, S.L., 1997, Plume–lithosphere interactions in the ocean basins: Constraints from the source mineralogy: Earth and Planetary Science Letters, v. 150, p. 245–260. doi:10.1016/S0012-821X(97)00089-7

D' Orazio, M., Agostini, S., Innocenti, F., Haller, M.J., Manetti, P., and Mazzarini, F., 2001, Slab window-related magmatism from southernmost South America: The Late Miocene mafic volcanics from the Estancia Glencross Area (52°S, Argentina–Chile): Lithos, v. 57, p. 67–89. doi:10.1016/S0024-4937(01)00040-8

Ernst, R.E., and Buchan, K.L., 2001, The use of mafic dike swarms in identifying and locating mantle plumes, in Ernst, R.E., and Buchan, K.L., eds., Mantle Plumes. Their identification through time, Volume Vol. 352: Geological Society of America, Special Paper, p. 247–265. doi:10.1130/0-8137-2352-3.247

Ernst, R.E., Buchan, K.L., and Palmer, H.C., 1995, Giant dyke swarms. Characteristics, distribution and geotectonic applications, in Baer, G., and Heimann, A., eds., Physics and Chemistry of Dykes: Rotterdam, Balkema, p. 3–21.

Foley, S., 1992, Vein-plus-wall-rock melting mechanisms in the lithosphere and the origin of potassic alkaline magmas: Lithos, v. 28, p. 435–453. doi:10.1016/0024-4937(92)90018-T

Geng, H.Y., Sun, M., Yuan, C., Xiao, W.J., Zhao, G.C., Zhang, L.F., Wong, K., and Wu, F.Y., 2009, Geochemical, Sr–Nd and zircon U–Pb-Hf isotopic studies of Late Carboniferous magmatism in the West Junggar, Xinjiang: Implications for ridge subduction?: Chemical Geology, v. 266, p. 364–389. doi:10.1016/j.chemgeo.2009.07.001

Geng, H.Y., Sun, M., Yuan, C., Zhao, G.C., and Xiao, W.J., 2011, Geochemical and geochronological study of early Carboniferous volcanic rocks from the West Junggar: Petrogenesis and tectonic implications: Journal of Asian Earth Sciences, v. 42, p. 854–866. doi:10.1016/j.jseaes.2011.01.006

George, R., and Rogers, N., 2002, Plume dynamics beneath the African plate inferred from the geochemistry of the Tertiary basalts of southern Ethiopia: Contributions to Mineralogy and Petrology, v. 144, p. 286–304. doi:10.1007/s00410-002-0396-z

George, R., Turner, S., Hawkesworth, C., Morris, J., Nye, C., Ryan, J., and Zheng, S-H., 2003, Melting processes and fluid and sediment transport rates along the alaska-aleutian arc from an integrated u-th-ra-be isotope study: Journal Of Geophysical Research: Solid Earth, v. 108, no. B5, p. 2252. doi:10.1029/2002JB001916

Gudmunsson, A., 1995, Infrastructure and mechanics of volcanic systems in Iceland: Journal of Volcanology and Geothermal Research, v. 64, p. 1–22. doi:10.1016/0377-0273(95)92782-Q

Halls, H.C., 1982, The importance and potential of mafic dyke swarms in studies of geodynamic processes: Geoscience Canada, v. 9, p. 145–154.

Han, B.F., Ji, J.Q., Song, B., Chen, L.H., and Zhang, L., 2006, Late Paleozoic vertical growth of continental crust around the Junggar Basin, Xinjiang, China (Part I): Timing of postcollisional plutonism: Acta Petrologica Sinica, v. 22, p. 1077–1086. [in Chinese with English abstract.]

Huang, B.C., Han, C.M., Sun, S., and Li, J.L., 2010, A review of the western part of the altaids: a key to understanding the architecture of accretionary orogens: Gondwana Research, v. 18, p. 253–273.

Kröner, A., Hegner, E., Lehmann, B., Heinhorst, J., Wingate, M.T.D., Liu, D.Y., and Ermelov, P., 2008, Palaeozoic arc magmatism in the Central Asian Orogenic Belt of Kazakhstan: SHRIMP zircon ages and whole-rock Nd isotopic systematics: Journal of Asian Earth Sciences, v. 32, p. 118–130. doi:10.1016/j.jseaes.2007.10.013

Langmuir, C.H., Klein, E.M., and Plank, T., 1992, Petrological systematics of mid-ocean ridge basalts: Constraints on melt generation beneath ocean ridges, in Morgan, J.P., Blackman, D.K., and Sinton, J.M., eds., Mantle flow and melt generation at mid-ocean ridges, Vol. 71, Washington, DC, AGU Geophys Monogr Series, p. 81–180. doi:10.1029/GM071p0183

Le Bas, M.J., Le Maitre, R.W., Streckeisen, A., and Zanettin, B., 1986, A chemical classification of volcanic rocks based on the total alkali-silica diagram: Journal of Petrology, v. 27, p. 745–750. doi:10.1093/petrology/27.3.745

Le Maitre, R.W., 2002, Igneous rocks: A classification and glossary of terms: Recommendations of international union of geological sciences subcommission on the systematics of igneous rocks: New York, Cambridge University Press, p. 236.

Li, X.H., Li, Z.X., Zhou, H.W., Liu, Y., and Kinny, P.D., 2002, U–Pb zircon geochronology, geochemistry and Nd isotopic study of Neoproterozoic bimodal volcanic rocks in the Kangdian Rift of South China: Implications for the initial rifting of Rodinia: Precambrian Research, v. 113, p. 135–154. doi:10.1016/S0301-9268(01)00207-8

Li, X.Z., Han, B.F., Ji, J.Q., Li, Z.H., Liu, Z.Q., and Yang, B., 2004, Geology, geochemistry and K–Ar ages of the Karamay basic-intermediate dike swarm from Xinjiang, China: Geochimica, v. 33, p. 574–584. [in Chinese with English Abstract.]

Ludwig, K.R., 2001, Isoplot/Ex, rev.2.49: A geochronological toolkit for Microsoft Excel, in Berkeley Geochronol, Center Special Publication, (1a): Berkeley, University of California, p. 55.

Luhr, J.F., and Haldar, D., 2006, Barren Island Volcano (NE Indian Ocean): Island-arc high alumina basalts produced by troctolite contamination: Journal of Volcanology and Geothermal Research, v. 149, p. 177–212. doi:10.1016/j.jvolgeores.2005.06.003

Ma, C., Xiao, W.J., Windley, B.F., Zhao, G.P., Han, C.M., Zhang, J.E., Luo, J., and Li, C., 2012, Tracing a subducted ridge–transform system in a late Carboniferous accretionary

prism of the southern Altaids: Orthogonal sanukitoid dyke swarms in Western Junggar, NW China: Lithos, v. 140, p. 152–165. doi:10.1016/j.lithos.2012.02.005

Maniar, P.D., and Piccoli, P.M., 1989, Tectonic discrimination of granitoids: Geological Society of America Bulletin, v. 101, p. 635–643. doi:10.1130/0016-7606(1989)101

McKenzie, D.P., and O' Nions, R.K., 1991, Partial melt distributions from inversion of rare earth element concentrations: Journal of Petrology, v. 32, p. 1021–1091. doi:10.1093/petrology/32.5.1021

Meng, L., Shen, P., Shen, Y.C., Liu, T.B., Song, G.X., Dai, H.W., Li, C.K., and Lang, Z.S., 2010, Igneous rocks geochemistry, zircon U–Pb age and its geological significance in the central section of Xiemisitai area, Xinjiang: Acta Petrologica Sinica, v. 26, p. 3047–3056. [in Chinese with English abstract.]

Park, J.K., Buchan, K.L., and Harlan, S.S., 1995, A proposed giant radiating dykes warm fragmented by the separation of Laurentia and Australia based on paleomagnetism of ca. 780 Ma mafic intrusions in western North America: Earth and Planetary Science Letters, v. 132, p. 129–139. doi:10.1016/0012-821X(95)00059-L

Patiño Douce, A.E., and Beard, J.S., 1995, Dehydration-melting of biotite gneiss and quartz amphibolite from 3 to 15 kbar: Journal of Petrology, v. 36, p. 707–738. doi:10.1093/petrology/36.3.707

Pearce, J.A., Harris, N.B.W., and Tindle, A.G., 1984, Trace element discrimination diagrams for the tectonic interpretation of granitic rocks: Journal of Petrology, v. 25, p. 956–983. doi:10.1093/petrology/25.4.956

Qi, J.Y., 1993, Geology and genesis of vein rock group in Western Zhunggar, Xinjiang: Acta Petrologica Sinica, v. 9, p. 288–299. [in Chinese with English Abstract.]

Rapp, R.P., and Watson, E.B., 1995, Dehydration melting of metabasalt at 8–32 kbar: Implications for continental growth and crust–mantle recycling: Journal of Petrology, v. 36, p. 891–931. doi:10.1093/petrology/36.4.891

Sharma, M., 1997, Siberian traps, in Mahoney, J.J., and Coffin, M.F., eds., Large Igneous provinces: Continental, oceanic, and planetary flood volcanism: Washington, D.C., American Geophysical Union, p. 273–295.

Shen, P., Shen, Y.C., Li, X.H., Pan, H.D., Zhu, H.P., Meng, L., and Dai, H.W., 2012, Northwestern Junggar Basin, Xiemisitai Mountains, China: A geochemical and geochronological approach: Lithos, v. 140, p. 103–118. doi:10.1016/j.lithos.2012.02.004

Shen, P., Shen, Y.C., Liu, T.B., Li, G.M., and Zeng, Q.D., 2008, Geology and geochemistry of the Early Carboniferous Eastern Sawur caldera complex and associated gold epithermal mineralization, Sawur Mountains, Xinjiang, China: Journal of Asian Earth Sciences, v. 32, p. 259–279. doi:10.1016/j.jseaes.2007.10.004

Sisson, T.W., Ratajeski, K., Hankins, W.B., and Glazner, A.F., 2005, Voluminous granitic magmas from common basaltic sources: Contributions to Mineralogy and Petrology, v. 148, p. 635–661. doi:10.1007/s00410-004-0632-9

Streckeisen, A.L., 1978, IUGS subcommission on the systematics of igneous rocks. Classification and nomenclature of volcanic rocks, lamprophyres, carbonatites and melilite rocks. Recommendations and suggestions: Neues Jahrbuchfür Mineralogie, Abhandlungen, v. 141, p. 1–14.

Sun, S.S., and McDonough, W.F., 1989, Chemical and isotopic systematics of oceanic basalt: Implications for mantle compositions and processes: Geological Society, London,

Special Publications, Vol. 42, p. 313–345. doi:10.1144/GSL.SP.1989.042.01.19

Tang, G.J., Wang, Q., Wyman, D.A., Li, Z.X.Z., Zhao, Z.H., and Yang, Y.H., 2012, Late Carboniferous high εNd(t)-εHf(t) granitoids, enclaves and dikes in western Junggar, NW China: Ridge subduction-related magmatism and crustal growth: Lithos, v. 84, p. 86–102. doi:10.1016/j.lithos.2012.01.025

Wang, F.Y., Liu, S.A., Li, S.G., and He, Y.S., 2013, Contrasting zircon Hf–O isotopes and trace elements between ore-bearing and ore-barren adakitic rocks in central-eastern China: Implications for genetic relation to Cu–Au mineralization: Lithos, v. 156–159, p. 97–111. doi:10.1016/j.lithos.2012.10.017

Wang, S.S., 1983, Age determinations of ^{40}Ar–^{40}K, ^{40}Ar–^{39}Ar and radiogenic ^{40}Ar released characteristics on K–Ar geostandards of China: Sciences Geological Sin, v. 4, p. 315–323. [in Chinese with English abstract.]

Wang, Z.Q., Jiang, X.M., Guo, J., Xu, F., Deng, X., Zhang, Q., Li, J., Niu, Q.Y., and Luo, Z.H., 2014, Discovery of the early paleozoic volcanic rocks in the Xiemisitai area of the West Junggar, Xinjiang: Geotectonica et Metallogenia, v. 38, p. 670–685. [in Chinese with English abstract.]

Weaver, B.L., and Tarney, J., 1981, The Scourie dyke suite: Petrogenesis and geochemical nature of the Proterozoic sub-continental mantle: Contributions to Mineralogy and Petrology, v. 78, p. 175–188. doi:10.1007/BF00373779

Wilson, M., 1989, Igneous Petrogenesis: London, Springer, Harper Collins Academic, p. 466.

Winchester, J.A., and Floyd, P.A., 1977, Geochemical discrimination of different magma series and their differentiation products using immobile elements: Chemical Geology, v. 20, p. 325–343. doi:10.1016/0009-2541(77)90057-2

Windley, B.F., Alexeiev, D., Xiao, W.J., Kröner, A., and Badarch, G., 2007, Tectonic models for accretion of the Central Asian Orogenic Belt: Journal of the Geological Society, v. 164, p. 31–47. doi:10.1144/0016-76492006-022

Wood, D.A., 1980, The application of a Th–Hf–Ta diagram to problems of tectonomagmatic classification and to establishing the nature of crustal contamination of basaltic lavas of the British Tertiary Volcanic Province: Earth and Planetary Science Letters, v. 50, p. 11–30. doi:10.1016/0012-821X(80)90116-8

Xiao, W.J., Han, C.M., Yuan, C., Sun, M., Lin, S.F., Chen, H.L., Li, Z.L., Li, J.L., and Sun, S., 2008, Middle Cambrian to Permian subduction-related accretionary orogenesis of North Xinjiang, NW China: Implications for the tectonic evolution of Central Asia: Journal of Asian Earth Sciences, v. 32, p. 102–117. doi:10.1016/j.jseaes.2007.10.008

Xiao, W.J., Windley, B.F., Allen, M.B., and Han, C.M., 2013, Paleozoic multiple accretionary and collisional tectonics of the Chinese Tianshan orogenic collage: Gondwana Research, v. 23, p. 1316–1341. doi:10.1016/j.gr.2012.01.012

Xiao, Wu, F., and Chen, B., 2000, Granitoids of the Central Asian Orogenic Belt and continental growth in the Phanerozoic: Transactions of the Royal Society of Edinburgh: Earth Sciences, v. 91, p. 181–193. doi:10.1130/0-8137-2350-7.181

Xu, Q.Q., Ji, J.Q., Han, B.F., Zhu, M.F., Chu, Z.Y., and Zhou, J., 2008, Petrology, geochemistry and geochronology of the intermediate to mafic dykes in northern Xinjiang since Late Paleozoic: Acta Petrologica Sinica, v. 24, p. 977–996. [in Chinese with English abstract.]

Xu, Z., Han, B.F., Ren, R., Zhou, Y.Z., Zhang, L., Chen, J.F., Su, L., Li, X.H., and Liu, D.Y., 2012, Ultramafic-mafic mélange, island arc and post-collisional intrusions in the Mayile Mountain, West Junggar, China: Implications for Paleozoic intra-oceanic subduction-accretion process: Lithos, v. 132, p. 141–161. doi:10.1016/j.lithos.2011.11.016

Yang, G.X., Li, Y.J., Santosh, M., Xiao, W.J., Yang, B.K., Tong, L.L., and Zhang, S.L., 2015, Alkaline basalts in the Karamay ophiolitic mélange, NW China: A geological, geochemical and geochronological study and implications for geodynamic setting: Journal of Asian Earth Sciences, v. 113, p. 110–125. doi:10.1016/j.jseaes.2014.08.017

Yang, G.X., Li, Y.J., Santosh, M., Yang, B.K., Zhang, B., and Tong, L.L., 2013, Geochronology and geochemistry of basalts from the Karamay ophiolitic mélange in West Junggar (NW China): Implications for Devonian–Carboniferous intra-oceanic accretionary tectonics of the southern Altaids: Geological Society of America Bulletin, v. 125, p. 401–419. doi:10.1130/B30650.1

Yang, G.X., Li, Y.J., Xiao, W.J., Sun, Y., and Tong, L.L., 2014, Petrogenesis and tectonic implications of the middle Silurian volcanic rocks in northern West Junggar, NW China: International Geology Review, v. 56, p. 869–884. doi:10.1080/00206814.2014.905214

Yin, J.Y., Chen, W., Xiao, W.J., Yuan, C., Sun, M., Tang, G.J., Yu, S., Long, X.P., Cai, K.D., Geng, H.Y., Zhang, Y., and Liu, X.Y., 2015b, Petrogenesis of early–permian sanukitoids from West Junggar, Northwest China: Implications for Late Paleozoic crustal growth in Central Asia: Tectonophysics, v. 662, p. 385–397. doi:10.1016/j.tecto.2015.01.005

Yin, J.Y., Chen, W., Xiao, W.J., Yuan, C., Windley, B.F., Yu, S., and Cai, K.D., 2017, Late Silurian–early Devonian adakitic granodiorite, A-type and I-type granites in NW Junggar, NW China: Partial melting of mafic lower crust and implications for slab roll-back: Gondwana Research, v. 43, p. 55–73. doi:10.1016/j.gr.2015.06.016

Yin, J.Y., Chen, W., Xiao, W.J., Yuan, C., Yu, S., Sun, J.B., Cai, K.D., and Long, X.P., 2016, The source and tectonic implications of late Carboniferous–early Permian A-type granites and dikes from the eastern Alataw Mountains, Xinjiang: Geochemical and Sr–Nd–Hf isotopic constraints: International Geology Review, p. 1–14. doi:10.1080/00206814.2016.1245161

Yin, J.Y., Chen, W., Yuan, C., Yu, S., Xiao, W.J., Long, X.P., Li, J., and Sun, J.B., 2015a, Petrogenesis of early carboniferous adakitic dikes, Sawur region, northern West Junggar, NW China: Implications for geodynamic evolution: Gondwana Research, v. 27, p. 1630–1645. doi:10.1016/j.gr.2014.01.016

Yin, J.Y., Chen, Y., Yuan, C., Zhang, Y.Y., Long, X.P., Yu, S., Zhang, Y., Li, J., and Sun, J.B., 2013a, Ages and tectonic implication of Late Paleozoic plutons in the West Junggar, North Xinjiang: Evidence from LA-ICPMS zircon geochronology: Geochimica, v. 42, no. 5, 415–430. [in Chinese with English abstract.]

Yin, J.Y., Long, X.P., Yuan, C., Sun, M., Zhao, G.C., and Geng, H.Y., 2013b, A late carboniferous slab window: Geochronological and geochemical evidence from mafic to intermediate dykes in West Junggar, NW China: Lithos, v. 175–176, p. 146–162. doi:10.1016/j.lithos.2013.04.005

Yin, J.Y., Yuan, C., Sun, M., Long, X.P., Zhao, G.C., and Geng, H.Y., 2010, Late carboniferous high- Mg dioritic dykes in Western Junggar, NW China: Geochemical features, petrogenesis and tectonic implications: Gondwana Research, v. 17, p. 145–152. doi:10.1016/j.gr.2009.05.011

Yuan, C., Sun, M., Wilde, S., Xiao, W.J., Xu, Y.G., Long, X.P., and Zhao, G.C., 2010, Post-collisional plutons in the Balikun area, East Chinese Tianshan: Evolving magmatism in response to extension and slab break-off: Lithos, v. 119, p. 269–288. doi:10.1016/j.lithos.2010.07.004

Zhang, Y., Chen, W., Chen, K.L., and Liu, X.Y., 2006, Study on the Ar–Ar age spectrum of diagenetic I/S and the mechanism of ^{39}Ar recoil loss-examples from the clayminerals of P–T boundary in Changxing, Zhejiang Province: Geological Review, v. 52, no. 4, 556–561. [in Chinese with English abstract.]

Zhang, Y.Y., and Guo, Z.J., 2010, New constraints on formation ages of ophiolites in northern Junggar and comparative study on their connection: Acta Petrologica Sinica, v. 26, p. 421–430. [in Chinese with English abstract.]

Zhao, L., and He, G.Q., 2013, Tectonic entities connection between West Junggar (NW China) and East Kazakhstan: Journal of Asian Earth Sciences, v. 72, p. 25–32. doi:10.1016/j.jseaes.2012.08.004

Zhou, T.F., Yuan, F., Fan, Y., Zhang, D.Y., Cooke, D., and Zhao, G.C., 2008, Granites in the Sawuer region of the west Junggar, Xinjiang Province, Chinageochronological and geochemical characteristics and their geodynamic significance: Geochronological and geochemical characteristics and their geodynamic significance: Lithos, v. 106, p. 191–206. doi:10.1016/j.lithos.2008.06.014

Zhu, Y.F., and Xu, X., 2006, The discovery of Early Ordovian ophiolite mélange in Taerbahatai Mts., Xinjiang, NW China: Acta Petrologica Sinica, v. 22, p. 2833–2842. [in Chinese with English abstract.]